Universal Magnetic Structure of the Half-Magnetization Phase in Cr-Based Spinels

M. Matsuda,[1] K. Ohoyama,[2] S. Yoshii,[2] H. Nojiri,[2] P. Frings,[3] F. Duc,[3] B. Vignolle,[3] G. L. J. A. Rikken,[3] L.-P. Regnault,[4] S.-H. Lee,[5] H. Ueda,[6] and Y. Ueda[6]

[1]*Quantum Beam Science Directorate, Japan Atomic Energy Agency (JAEA), Tokai, Ibaraki 319-1195, Japan*
[2]*Institute for Materials Research, Tohoku University, Katahira, Sendai 980-8577, Japan*
[3]*Laboratoire National des Champs Magnétiques Intenses, UPR3228 CNRS-INSA-UJF-UPS, Grenoble & Toulouse, France*
[4]*CEA-Grenoble, INAC-SPSMS-MDN, 17 rue des Martyrs, 38054 Grenoble Cedex 9, France*
[5]*Department of Physics, University of Virginia, Charlottesville, Virginia 22904-4714, USA*
[6]*The Institute for Solid State Physics, The University of Tokyo, Kashiwa, Chiba 277-8581, Japan*

(Received 16 July 2009; published 26 January 2010)

Using an elastic neutron scattering technique under a pulsed magnetic field up to 30 T, we determined the magnetic structure in the half-magnetization plateau phase in the spinel $CdCr_2O_4$. The magnetic structure has a cubic $P4_332$ symmetry, which is the same as that observed in $HgCr_2O_4$. This suggests that despite their different zero-field ground states a universal field-induced spin-lattice coupling mechanism is at work in the Cr-based spinels.

DOI: 10.1103/PhysRevLett.104.047201 PACS numbers: 75.30.Kz, 75.25.−j, 75.50.Ee

When an external magnetic field is applied to strongly interacting spin systems, novel collective phenomena may arise [1]. A well-known example is the field-induced condensation of magnons in quantum magnets [2]. Another is the field-induced fractional magnetization plateau observed in frustrated magnets [3]. Interest in the latter system stems from the degenerate ground state due to the triangular motif of the magnetic lattice [4,5]. For instance, for a tetrahedron made of four isotropic classical spins, any spin configuration with a total zero spin can be the ground state. There is an infinite number of such configurations that satisfy the criterion. When such tetrahedra are arranged in a corner-sharing network, sometimes called the pyrochlore lattice, the ground state degeneracy becomes macroscopic, and exotic magnetic properties are expected at low temperatures [6–8]. If the spin degree of freedom is coupled with the lattice or orbital degree of freedom, the system can undergo a phase transition at low temperature into a crystallographically distorted and magnetic ordered state [9–17]. When an external magnetic field (H) is applied to the ordered state, the fractional magnetization phase appears and is associated with each tetrahedron having majority (minority) spins aligned parallel (antiparallel) to H. There can be many ways of organizing the majority and minority spins over the entire lattice, and how a certain structure can be stabilized over a wide range of H and whether or not a universal ground state for each type of frustrated lattice and Hamiltonians exists are of issue.

The Cr-based spinels ACr_2O_4 (A = Hg, Cd, and Zn) can provide good model systems with frustrating spin Hamiltonians. It has a cubic $Fd\bar{3}m$ crystal structure at room temperature where the magnetic Cr^{3+} (nominally t_{2g}^3; $s = 3/2$) ions without orbital degeneracy form the pyrochlore lattice. Furthermore, due to the edge-sharing network of CrO_6 nearly octahedra, the direct hybridization of neighboring t_{2g}-t_{2g} orbitals can lead to strongly antiferromagnetic nearest-neighbor (NN) exchange interactions. On the other hand, the CrO_6 octahedron is not perfect but trigonally distorted, which can lead to t_{2g}-e_g hybridization that results in ferromagnetic NN interactions and stronger further nearest-neighbor interactions [18]. Experimentally, large Curie-Weiss temperatures were observed, $\Theta_{CW} = -32$ K (Hg), -88 K (Cd), and -390 K (Zn), indicating overall strong antiferromagnetic interactions. The system remains in a spin-liquid state down to temperatures (T) much lower than $|\Theta_{CW}|$, indicative of the presence of strong frustration [3]. Upon further cooling, it undergoes a transition at 6 K (Hg), 7.8 K (Cd), and 12.5 (Zn) due to spin-lattice coupling into a magnetically long range ordered state [9,10,19]. The nature of the magnetic structure and lattice distortion is different for different A site ions: the symmetry of the low T crystal structure is orthorhombic $Fddd$, tetragonal $I4_1/amd$, and tetragonal $I\bar{4}m2$ for Hg, Cd, and Zn, respectively. Their magnetic structures also have different characteristic wave vectors: two commensurate wave vectors $\mathbf{Q}_m = (1, 0, 1/2)$, (1,0,0) for Hg [19], a single incommensurate $\mathbf{Q}_m = (0, \delta, 1)$ for Cd [10], and two commensurate $\mathbf{Q}_m = (1/2, 1/2, 0)$, (1, 0, 1/2) for Zn [20]. These may tell us that the ratios of the exchange coupling constants, Js, are different for different A ions. A recent first-principle calculation study [18] showed that Js can vary dramatically depending on the A site ion: for Zn and Cd the nearest neighbor J_{NN} is dominant, while for Hg the third neighbor interaction J_3 is dominant.

When an external field, H, is applied, the Cr spinel undergoes a phase transition into a half-magnetization plateau phase at $H_{c1} = 10$ T for Hg, 28 T for Cd, and 120 T for Zn [3,21,22], suggesting that each tetrahedron has three up (majority) and one down (minority) spins (3:1

constraint). The field-induced magnetic and chemical structure of $HgCr_2O_4$ with the lowest H_{c1} was determined, since its H_{c1} is within the steady magnet capability, ~17.5 T, available at neutron facilities, to have the $P4_332$ symmetry or its mirror image $P4_132$ [19].

The magnetic-field-induced phases of the other Cr spinels have been impossible because of their high critical fields that are beyond the current *steady* magnet technology. This technological limitation prevented us from addressing an important issue: whether the nature of the field-induced phase in the Cr spinels varies with different A ions as it does for the zero-field spin-lattice coupling or whether it can be universal. Since the spin Hamiltonian varies with the A site ion, it is natural to expect that the field-induced spin-lattice coupling will also depend on the A-site ion. Here we will show that this is not the case by utilizing a new *pulsed* magnet capability up to 30 T that is now available at neutron scattering facilities to study the half-magnetization plateau phase of $CdCr_2O_4$. We show that for $H > H_{c1} = 28$ T, the incommensurate magnetic peaks that exist in $CdCr_2O_4$ for $H = 0$ disappear while new peaks appear with the characteristic wave vector of $\mathbf{Q}_m = (1, 0, 0)$ but not at the $(2, \bar{2}, 0)$ point. This clearly demonstrates that the half-magnetization plateau phase of $CdCr_2O_4$ has the same $P4_332$ magnetic structure as that of $HgCr_2O_4$. Our results indicate that the observed $P4_332$ state is the generic ground state of the field-induced phase of the Cr-spinels despite their different zero-field spin-lattice states.

A single crystal that has a shape of a thin plate (~4 mm × 4 mm × 0.2 mm) and weighs ~40 mg was used. Since natural Cd has a large neutron absorption cross section, a single crystal enriched with ^{114}Cd isotope was used for our measurements. The elastic neutron scattering experiments were carried out on the thermal neutron triple-axis spectrometers IN22 at Institut Laue-Langevin (ILL). The incident and final neutron energies were fixed to $E_i = 34.8$ meV. Contamination from higher order neutrons was effectively eliminated by a pyrolytic graphite filter. The 40 mg single crystal was mounted with the [111] and $[1\bar{1}0]$ axes in the horizontal scattering plane. A small magnet coil made of CuAg wire was mounted surrounding the crystal on a cryostat insert and the apparatus was cooled in a standard ^{4}He cryostat [23–25]. The magnet coil in the cryostat was connected to a transportable capacitor bank that resided outside of the cryostat. A half-sine shaped pulsed magnetic field of 8 msec duration was generated by using a capacitor bank [26]. The magnetic field was measured by a set of pickup coils installed around the sample. The magnet coil limited the accessible scattering angle below 30°, which allowed us to reach only two commensurate reflections at (1, −1, 0) and (2, −2, 0) and incommensurate peaks around (1, −1, 0). The pulsed measurements were performed more than 100 times at each reflection to obtain reasonable statistics.

At zero magnetic field, $CdCr_2O_4$, shows a spiral magnetic order with a single characteristic wave vector of $\mathbf{Q}_m = (0, \delta, 1)$ or $(\delta, 0, 1)$ where $\delta \sim 0.09$, accompanied by a tetragonal distortion below $T_N = 7.8$ K. [10,27] Thus, the incommensurate (IC) wave vectors within the accessible scattering angle of 30° are $(1, -1 \pm \delta, 0)$ and $(1 \pm \delta, -1, 0)$. Even though these peaks are out of the scattering plane separated by ~0.025 Å^{-1}, they could be detected in our measurements because the full width of the half maximum of the vertical instrumental resolution was 0.144 Å^{-1}. We performed elastic scans around the $(1, -1, 0)$ point and found superlattice peaks at four positions shown in Fig. 1(a). In Fig. 1(b), a typical elastic scan taken along the $(1, 1, 1)$ direction centered at $(1.04, -1.04, 0)$ show two peaks at $\mathbf{k}_1$ and $\mathbf{k}_2$ of Fig. 1(a). The four peak positions, $\mathbf{k}_1$, $\mathbf{k}_2$, $\mathbf{k}_3$, and $\mathbf{k}_4$, correspond to the IC peaks at $(1.09, -1, 0)$, $(1, -1.09, 0)$, $(1, -0.91, 0)$, and $(0.91, -1, 0)$ projected on the scattering plane.

Figure 2(a) shows the time dependence of the elastic neutron scattering intensity measured at the IC magnetic peak of $(1.0675, -1.0125, 0.0275)$ at 2.5 K. The peak intensity initially decreases gradually up to 1 ms that corresponds to $H = 8$ T and remains constant at 20 counts per 200 pulses up to 3 ms, after which the intensity sharply decreases to background level. The 3 ms time corresponds to $H = 28$ T, which is consistent with the critical field observed in the previous bulk magnetization measurements [3]. The magnetic field reaches the maximum 29.6 T at 3.9 ms after which H decreases. The IC magnetic signal remains zero up to 4.6 ms ($H = 28$ T) after which the intensity increases back to the intermediate level at $H = 8$ T but not to the original intensity at $H = 0$ T. The hysteretic behavior originates from the magnetic domain

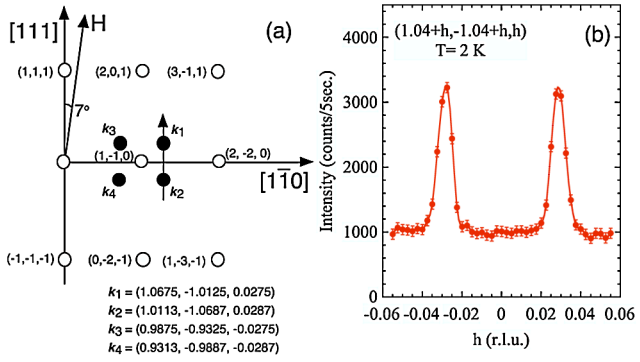

FIG. 1 (color online). (a) A schematic diagram of the [111] and $[1\bar{1}0]$ horizontal scattering plane that was used for our neutron scattering measurements. The external pulsed magnetic field, H, was applied horizontally 7° away from the [111] direction as shown by an arrow. The open circles represent commensurate wave vector positions, and the filled circles represent the $(0, \delta, 1)$ incommensurate magnetic Bragg positions observed for zero magnetic field. (b) Our elastic neutron scattering data taken with $H = 0$ at 2 K along the $(1.04 + h, -1.04 + h, h)$ as shown by an arrow in (a).

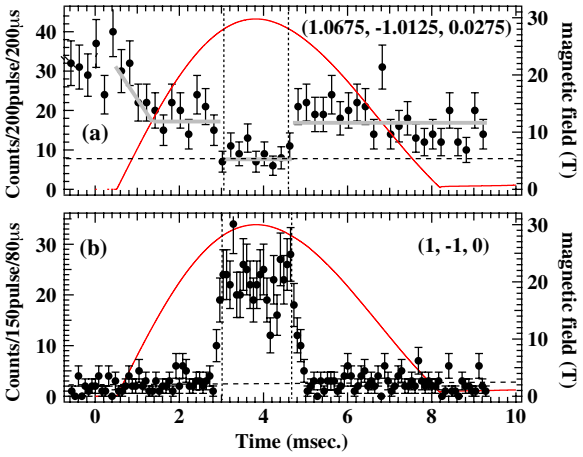

FIG. 2 (color online). Time dependence of the magnetic field [solid (red) lines] and neutron counts (●) measured at (1.0675, −1.0125, 0.0275) and (1, −1, 0) reflections at the initial temperature $T = 2.5$ K. The corresponding magnetic field is shown on the right y axis. The measurements were performed over 200 and 150 magnetic-field pulses for (1.0675, −1.0125, 0.0275) and (1, −1, 0) reflections, respectively, and the data were summed. Binning times were 200 and 80 μs for (1.0675, −1.0125, 0.0275) and (1, −1, 0) reflections, respectively. The vertical dotted lines are drawn at the times corresponding nominally to the critical field, $H_c = 28$ T. The horizontal dashed lines represent the background levels determined at wave vectors away from the reflection positions. The gray thick lines are guides for the eye.

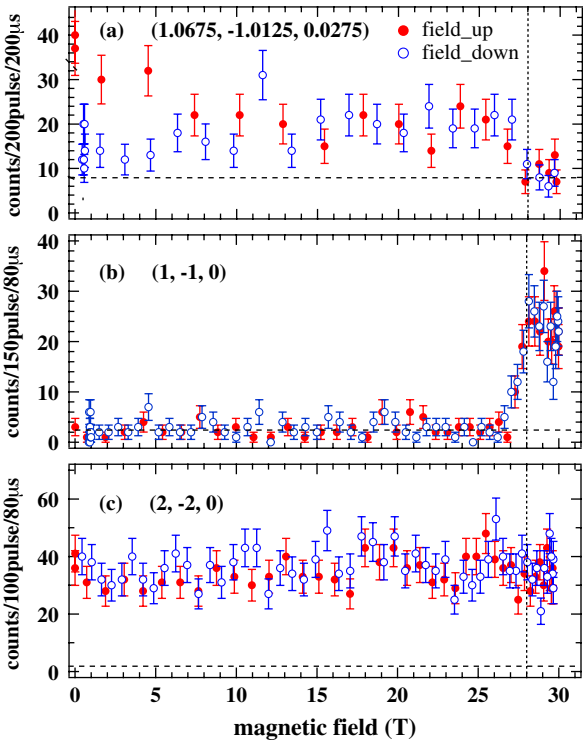

FIG. 3 (color online). Magnetic-field dependence of the peak intensity of the (a) (1.0675, −1.0125, 0.0275), (b) (1, −1, 0), and (c) (2, −2, 0) reflections measured at $T = 2.5$ K with the ascending (●) and descending (○) field. For better statistics, binning times were 200, 80, and 80 μs for (1.0675, −1.0125, 0.0275), (1, −1, 0), and (2, −2, 0) reflections, respectively. The vertical dotted lines are drawn at the times corresponding nominally to the critical field, $H_c = 28$ T. The horizontal dashed lines represent background intensity.

orientation and is consistent with the previous result [27]. While waiting about 8 min for the next current pulse, the sample was warmed up to 20 K $> T_N$ and cooled back down to 2.5 K to recover the original zero-field intensity.

In order to find out to where the elastic magnetic intensity that disappeared at the IC wave vector for fields $H >$ 28 T transferred, we performed similar measurements at a commensurate $\mathbf{Q} = (1, -1, 0)$ position. Figures 2(b) and 3(b) show the results as a function of time and field. When a magnetic field was injected, no signal was initially observed at (1, −1, 0) for 3 ms at which point the intensity suddenly increased due to the first-order nature of the field-induced phase transition. The commensurate magnetic intensity remained nonzero over exactly the same range of time (and field) over which the IC magnetic signal went down to zero. Our results indicate that as $CdCr_2O_4$ enters the half-magnetization plateau state upon application of an external magnetic field, the magnetic structure changes from the incommensurate spiral to a commensurate collinear spin structure with $\mathbf{Q}_m = (1, 0, 0)$. Once the 3:1 constraint is imposed, the (100)-type reflections are consistent with two nonequivalent spin configurations for the pyrochlore lattice: one with cubic $P4_332$ symmetry [Fig. 4(a)] and the other with rhombohedral $R\bar{3}m$ symmetry [Fig. 4(b)] [19]. To distinguish between the two models, we also performed similar pulsed field measurements at $(2, \bar{2}, 0)$ at which point the $R\bar{3}m$ structure should produce magnetic Bragg scattering while the $P4_332$ structure would not. At $H = 0$, nuclear Bragg intensity is observed at $(2, \bar{2}, 0)$. As shown in Fig. 3(c), the $(2, \bar{2}, 0)$ intensity does not change as the system enters the half-magnetization phase. Thus, we conclude that the half-magnetization spin state of $CdCr_2O_4$ has the same $P4_332$ spin structure

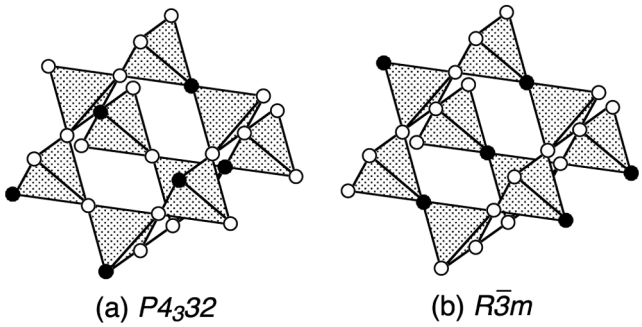

FIG. 4. Magnetic structures with cubic $P4_332$ (a) and rhombohedral $R\bar{3}m$ (b) symmetries. Open and filled circles represent up and down spins, respectively. Each tetrahedron has three up and one down spins.

as observed in $HgCr_2O_4$. This is rather surprising because the two systems have quite different ground states at $H = 0$.

Why is the $P4_332$ spin structure favored as the ground state of the half-magnetization phase in Cr spinels? There are many ways of arranging the pyrochlore lattice with tetrahedra holding the 3:1 constraint because there is considerable freedom in choosing the location of the down spin on each tetrahedron. Crucial information comes from the fact that the crystal structure also changes at the field-induced phase transition. Previous combined neutron and synchrotron x-ray measurements on $HgCr_2O_4$ showed that at the field-induced phase transition, the crystal structure indeed becomes cubic with the $P4_332$ symmetry [19]. Recent synchrotron x-ray diffraction experiments on $CdCr_2O_4$ under pulsed magnetic field showed that the crystal structure of the half-magnetization phase is cubic as well [28]. Thus, the plateau phase involves a field-induced spin-lattice coupling. It is to be emphasized that the two systems have *different* zero-field ground states, suggesting their effective spin Hamiltonians, $\mathcal{H}$, are different in details. This is consistent with a recent first-principle calculation study on the ACr_2O_4 [18] that showed that for $A =$ Zn and Cd, J_{NN} is dominant while for $A =$ Hg, J_3 is dominant. Thus it is surprising that $CdCr_2O_4$ and $HgCr_2O_4$ have the exact same field-induced state. One can understand this by considering which exchange interaction bonds would be most severely distorted in the cubic $P4_332$ crystal structure. In the $P4_332$ structure, every line connecting the two nearest-neighboring minority (down) spins is bent, affecting J_{NN} the most. This suggests that their effective Hamiltonians must have a common term of an elastic energy of spins involving J_{NN} that governs the physics of the field-induced phase transition. A theory called an Einstein phonon model has indeed been proposed in which the Hamiltonian consists of the NN exchange interaction that is sensitive to the NN bond distance minus an elastic energy associated with the displacements of the magnetic atoms. They showed that maximizing the displacements or minimizing the Hamiltonian occurs in a unique bending pattern of tetrahedra that has the $P4_332$ symmetry [29]. This supports our conclusion that the Cr spinels most likely have the common spin-elastic energy term in their Hamiltonians which leads to the universal behavior under an external magnetic field, regardless of their differences in their spin Hamiltonians.

In summary, our elastic neutron scattering experiments on a single crystal of $CdCr_2O_4$ under a pulsed magnetic field up to 30 T showed that the Cr spinels, ACr_2O_4 with nonmagnetic A ions, have a unique field-induced half-magnetization state, regardless of their different zero-field ground states. Our study demonstrates that with the new pulsed magnet capability up to 30 T now available at neutron facilities, new research opportunities in the field of frustrated magnetism open up. To understand the observed universal behaviors of the Cr spinels under an external magnetic field requires theoretical efforts on the field-induced spin-lattice coupling.

This work was partially supported by a Grant-in-Aid for Scientific Research on priority areas "High Field Spin Science in 100T" (No. 451), "Novel States of Matter Induced by Frustration" (No. 19052004 and No. 19052008) from the Ministry of Education, Culture, Sports, Science, and Technology (MEXT) of Japan, and by the ICC-IMR Center of Tohoku University. S. H. L. is supported by the U.S. Department of Energy, Office of Basic Energy Sciences, Division of Materials Sciences and Engineering under No. DE-FE02-07ER46384.

[1] S. Sachdev, Nature Phys. **4**, 173 (2008).
[2] T. Nikuni *et al.*, Phys. Rev. Lett. **84**, 5868 (2000).
[3] H. Ueda *et al.*, Phys. Rev. Lett. **94**, 047202 (2005).
[4] S. T. Bramwell and M. J. P. Gingras, Science **294**, 1495 (2001).
[5] R. Moessner and A. P. Ramirez, Phys. Today **59**, No. 2, 24 (2006).
[6] R. Moessner and J. T. Chalker, Phys. Rev. Lett. **80**, 2929 (1998).
[7] B. Canals and C. Lacroix, Phys. Rev. Lett. **80**, 2933 (1998); Phys. Rev. B **61**, 1149 (2000).
[8] S.-H. Lee *et al.*, Nature (London) **418**, 856 (2002).
[9] S.-H. Lee *et al.*, Phys. Rev. Lett. **84**, 3718 (2000).
[10] J.-H. Chung *et al.*, Phys. Rev. Lett. **95**, 247204 (2005).
[11] Y. Yamashita and K. Ueda, Phys. Rev. Lett. **85**, 4960 (2000).
[12] O. Tchernyshyov, R. Moessner, and S. L. Sondhi, Phys. Rev. Lett. **88**, 067203 (2002).
[13] D. I. Khomskii and T. Mizokawa, Phys. Rev. Lett. **94**, 156402 (2005).
[14] Y. Ueda, N. Fujiwara, and H. Yasuoka, J. Phys. Soc. Jpn. **66**, 778 (1997).
[15] S.-H. Lee *et al.*, Phys. Rev. Lett. **93**, 156407 (2004).
[16] H. Tsunetsugu and Y. Motome, Phys. Rev. B **68**, 060405 (R) (2003).
[17] O. Tchernyshyov, Phys. Rev. Lett. **93**, 157206 (2004).
[18] A. N. Yaresko, Phys. Rev. B **77**, 115106 (2008).
[19] M. Matsuda *et al.*, Nature Phys. **3**, 397 (2007).
[20] S. Ji *et al.*, Phys. Rev. Lett. **103**, 037201 (2009).
[21] H. Ueda *et al.*, Phys. Rev. B **73**, 094415 (2006).
[22] E. Kojima *et al.*, J. Phys. Conf. Ser. **145**, 012023 (2009).
[23] K. Ohoyama *et al.*, J. Phys. Conf. Ser. **51**, 506 (2006).
[24] K. Ohoyama *et al.*, J. Magn. Magn. Mater. **310**, e974 (2007).
[25] S. Yoshii *et al.*, Phys. Rev. Lett. **103**, 077203 (2009).
[26] P. Frings *et al.*, Rev. Sci. Instrum. **77**, 063903 (2006).
[27] M. Matsuda *et al.*, Phys. Rev. B **75**, 104415 (2007).
[28] T. Inami *et al.*, J. Phys. Conf. Ser. **51**, 502 (2006).
[29] D. L. Bergman *et al.*, Phys. Rev. B **74**, 134409 (2006).